Title
STRUCTURAL STUDIES OF XENON FLUORIDE COMPLEXES

Author
Morrell, Barbara K.

Publication Date
1971-09-01

STRUCTURAL STUDIES OF XENON FLUORIDE COMPLEXES

Barbara K. Morrell

September 1971

AEC Contract No. W-7405-eng-48

DISCLAIMER

STRUCTURAL STUDIES OF XENON FLUORIDE COMPLEXES

Contents

STRUCTURAL STUDIES OF XENON FLUORIDE COMPLEXES

Barbara K. Morrell

Inorganic Materials Research Division, Lawrence Berkeley Laboratory
and Department of Chemistry; University of California
Berkeley, California

ABSTRACT

Previous x-ray structural work has shown the compounds $F_{11}XePt$ and $F_{11}XeAs$ to be XeF_5^+ salts. The structure of the arsenic compound, however, was never completed to satisfaction and remains unpublished. In the structure of the platinum compound, the residual value of 0.14 was sufficiently high to allow the possibility of the incorrect space group having been chosen. Even allowing the correctness of these structures, however, their precision were sufficiently low that they failed to provide decisive information on one important bonding feature. The relative bond lengths of the apical and equatorial F-Xe bonds in the XeF_5^+ cation has relevance to the various bonding models for this and related species. The previous structures did not establish significant differences for these bonds.

X-ray powder data and infrared spectra of the ruthenium and iridium compounds suggested they might be isostructural with the platinum complex. Furthermore, since crystalline XeF_6 can be formulated as $XeF_5^+F^-$, all the 1:1 adducts are probably XeF_5^+ salts. In an endeavor to obtain a more precise structure, the ruthenium complex $F_{11}XeRu$ was selected. This compound provides for a greater relative contribution of the fluorine atoms to the x-ray scattering than in the platinum compound

because of the lower scattering factor of ruthenium relative to platinum. The lower x-ray absorption by the ruthenium compound was also advantageous.

The crystal structure of the ruthenium compound has been determined with sufficient precision to establish that the axial Xe-F bond in XeF_5^+ is significantly shorter than the equatorial. The bond lengths are compatible with simple bonding models.

In an effort to explore the relative fluoride ion donor properties of XeF_2 and XeF_6 toward RuF_5 and the possibility of molecule-ion adducts, as already observed in $XeF_2 \cdot XeF_6 \cdot AsF_5$ and $XeF_2 \cdot 2XeF_6 \cdot 2AsF_5$, the system $XeF_2/XeF_5^+RuF_6^-$ was investigated. No mixed valence compounds were obtained, nor was XeF_6 displaced from $XeF_5^+RuF_6^-$ by XeF_2. These results support predictions based on previous experimental evidence.

I. INTRODUCTION

The chemistry of noble gas compounds evolved in 1962 as a result of Bartlett's discovery that xenon gas could be oxidized with platinum hexafluoride vapor to produce a platinum complex fluoride.[1] Since then, many new types of xenon compounds have been prepared by combining the noble gas atom with highly electronegative ligands.[2] In addition to its high electronegativity and small size, thermodynamic considerations indicate fluorine to be the most favorable ligand with which to prepare noble gas compounds.[3] Fluorine will form stronger bonds with noble gases, and its compounds will be thermodynamically more stable than those formed from other halogens, oxides, or other highly electronegative ligands.[4]

Xenon difluoride was originally synthesized by two independent groups,[5,6] and has since been prepared by various methods.[7,8,9] Soon afterward, xenon tetrafluoride[10] and xenon hexafluoride[11,12,13,14] were reported.

A variety of XeF_2 complexes have been prepared, and the difluoride established as a fluoride ion donor in providing both $Xe_2F_3^+$ and XeF^+ salts. It has been demonstrated that the tetrafluoride is a much inferior fluoride ion donor, but, curiously, the hexafluoride is a better fluoride ion donor than the difluoride.[15]

Reported derivatives of the hexafluoride include XeF_6AsF_5,[16,17,18] XeF_6SbF_5,[19] XeF_6PtF_5,[20,21] XeF_6IrF_5,[15] XeF_6BF_3,[16] XeF_6GeF_4,[22] and XeF_6RuF_5.[23]

The two XeF_6MF_5 structures that have been done to date indicate that these compounds are XeF_5^+ salts and suggest apical Xe-F bond shortening. The data, however, are inconclusive on the basis of

reported standard deviations. Previous x-ray structural work on species geometrically similar to the XeF_5^+ cation do show shortening of the Xe-F apical bond. These results, as well as the two previous XeF_5^+ structure results, are tabulated below in Table I.

TABLE I.

Bond lengths (Å) and Bond Angles (degrees) with standard deviations given in parentheses.

	TeF_5^-	IF_5	$(XeF_5^+)PtF_6^-$	$(XeF_5^+)AsF_6^-$
M-F_a	1.84(2)	1.817(10)	1.81(8)	1.79
M-F_b	1.96(2)	1.873(5)	1.88(8)	1.82
Fa-M-Fb	78.9(1.6)	80.9(2)	79.0(4)	70.4
Reference	24	25	21	26

It was considered likely that the ruthenium XeF_5^+ structure analysis would eliminate existing ambiguities.

Earlier work has shown that xenon difluoride forms molecular adducts with XeF_5^+ species. To date Bartlett and Wechsberg have prepared and isolated the 1:1:1 and the 1:2:2 adducts in the XeF_2/XeF_6/AsF_5 system.[27] These were prepared by simply fusing the neat components in appropriate molar ratios in Kel-F tubes under nitrogen atmosphere at 85°C.[27] Raman data showed these to be molecular complexes, the structures of which are compatible with xenon difluoride bond polarity. The occurrence of molecular XeF_2 in the $XeF_5^+AsF_6^-$ structure adds further support to the greater fluoride ion donor ability of XeF_6 as compared to XeF_2.[27] It was of interest to

investigate the possibility of XeF_2 adducts in the XeF_6/RuF_5 system to see if XeF_2 and XeF_6 exhibit similar F^- donor properties in this transition metal system.

II. EXPERIMENTAL

A. General Techniques

Moisture and air sensitivity as well as the high oxidizing power of xenon fluoride complexes require special handling. Compounds were prepared on a metal vacuum system as previously described,[28] in Kel-F or monel vessels. Sample manipulation was carried out in a Vacuum Atmospheres Corporation Dri-Lab supplied with nitrogen as the inert gas.

For x-ray powder and single crystal work, the specimens were packed in dry quartz capillaries in the Dri-Lab atmosphere, sealed temporarily with Kel-F grease, then sealed permanently with an oxygen torch upon removal to the air. A shortage of commercially made, thin-walled quartz capillaries necessitated hand blowing our own. These handmade capillaries later caused problems with data collection; their thick, and uneven walls resulted in very high and inconsistent background counts.

Samples used in taking infrared spectra were sealed between silver chloride windows of a prefluorinated Kel-F infrared cell.

B. Preparation of $F_{11}RuXe$

This compound was first successfully prepared by Sladky from a xenon, fluorine, RuF_5 mixture using an excess of fluorine gas.[29] As a simple alternative, we synthesized the compound by fluorinating a sample of XeF_2RuF_5 prepared earlier in this laboratory by M. Geniss.

Preparation. Using a 1 liter ballast, fluorine (460 torr) was largely transferred to a prefluorinated 45 ml bomb at -196°C containing $XeF^+RuF_6^-$ (1.00 g.). The bomb was heated 14 hours in a sand bath at 350°C and slowly cooled to room temperature. Excess fluorine was pumped off at -196°C.

Characterization. The resulting compound remaining in the bomb was a pale green powder (m.p. 136°C) which gave an x-ray powder pattern corresponding exactly to that obtained previously by Sladky for $XeF_6 \cdot RuF_5$. The infrared spectrum of the powder between AgCl plates showed strong lines at 699 and 607 cm^{-1}. Other characteristic bands appeared at 675, 295, and 222 cm^{-1}, in order of decreasing intensities. These results are also in agreement with the findings of Garrison.[30] On the basis of frequency and intensity, it is possible that the 698 cm^{-1} band corresponds to lines at 687 cm^{-1} in the iridium compound, and to 677 cm^{-1} in the platinum analogue, all of which are the derivatives of the ν_3 octahedral mode for the MF_6^- species.

C. XeF_2 Complexes with $XeF_5^+RuF_6^-$

Preparation of a molecule-ion adduct of XeF_2 with $XeF_5^+RuF_6^-$ was attempted by fusion of the neat components with varying conditions of pressure and temperature.

Preparation. Following the procedure outlined in the AsF_5 complex synthesis,[27] XeF_2 (1 mmole) and $XeF_5^+RuF_6^-$ (1 mmole) were crushed and mixed together in the Dri-Lab using an agate mortar and pestal. The mixture was transferred to a Kel-F tube and shaken vigorously to further enhance homogeneous mixing. The tube was heated to a temperature of 105°C for 5 hours under nitrogen atmosphere in an oil bath. Since the color of the substance as seen through the tube changed from pale to dark green, it was assumed a melt had been obtained at 105°C. After slowly cooling the tube to room temperature, the product appeared unchanged from the starting material. Powder patterns of this product matched those of $XeF_5^+RuF_6^-$. No XeF_2 lines were observed.

Two subsequent attempts at fusing the neat components at 120°C and 140°C produced similar powder patterns of very intense $XeF_5^+RuF_6^-$ lines. In both cases there was no indication of the presence of molecular XeF_2. Xenon difluoride had apparently sublimed out, and large white crystals characteristic of xenon difluoride adhered to the tops of the Kel-F tubes. One such crystal was mounted on a precession camera and identified as the XeF_2 tetragonal species.

Finally, the synthesis was attempted using HF solvent to insure homogeneous mixing of the components. The powder pattern

of the product showed no evidence of complex formation or any XeF_2-ion interaction.

Failure to produce a new phase from the $XeF_2/XeF_5^+RuF_6^-$ mixtures by these methods indicates that there is unlikely to be a strong interaction between XeF_2 and XeF_5^+ in the fluororuthenate.

III. THE CRYSTAL STRUCTURE OF $F_{11}XeRu$

A. Single Crystal Growth

Well-formed single crystals of $F_{11}XeRu$ were grown in sealed quartz capillaries by sublimation. Clear tablet-shaped crystals sublimed *in situ* after heating the capillaries for three to five days at 120°C in a Variac controlled furnace designed and built by D. Gibler and illustrated in Figure 1. The nichrome wire was coiled in such a way as to provide a temperature gradient.

The single crystal chosen for this x-ray work, however, was grown by *in situ* sublimation under reduced pressure. The capillary was sealed under 1 atmosphere nitrogen pressure in the dry box. Apparatus for this procedure consisted of simply attaching to a vacuum line a Pyrex tube containing unsealed quartz capillaries loaded with minute amounts of the ruthenium salt. With the tube under dynamic vacuum, the temperature was controlled at approximately 94°C. Figure 2 illustrates this apparatus.

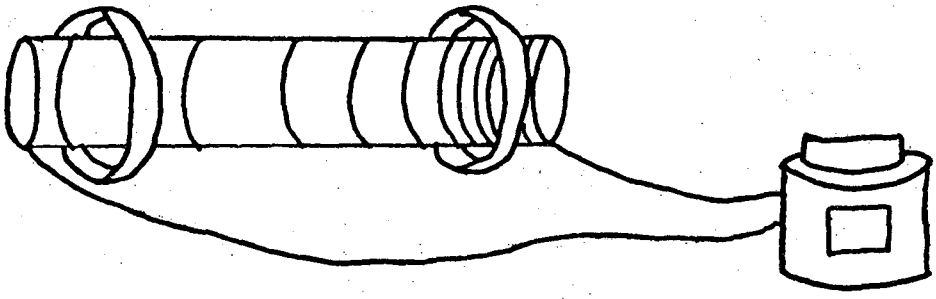

Figure 1. Variac controlled Pyrex furnace. Nichrome wire provides temperature gradient over which crystals sublime.

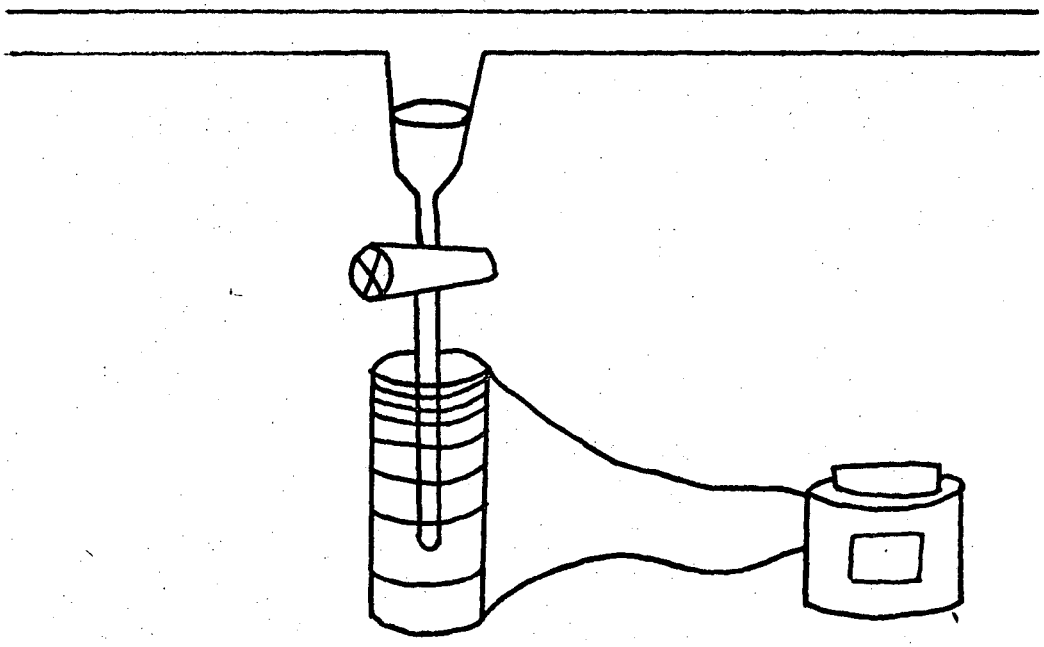

Figure 2. Apparatus for growing crystals in near-vacuum atmosphere. Sample is kept in evacuated tube as it is being heated by a Variac controlled furnace.

B. Crystal Data

A clear, tablet-shaped crystal of dimensions 0.15 x 0.06 x 0.10 mm fixed to the sides of a sealed quartz capillary was oriented on a Nonius goniometer head with its c axis parallel to the rotation axis of the capillary. From film precession and Weissenberg photographs, the space group and cell dimensions were determined. These photographs exhibited orthorhombic symmetry with systematic absences $0k\ell$, $k + \ell = 2n$ and $hk0$, $h = 2n$. Crystal cell dimensions from the films were refined by a least squares analysis of high angle diffractometer data to be:

$$a = 17.771(10)\ \text{Å}$$

$$b = 8.206(10)\ \text{Å}$$

$$c = 5.617(10)\ \text{Å}$$

The compound was refined in the centrosymmetric space group Pnma (number 62) after spot-checking intensities of reflections in $hk\ell$ and $\bar{h}k\ell$ made the non-centrosymmetric space group $Pna2_1$ less likely. For this compound, $U = 773.027\ \text{Å}^3$. For four formula units in the cell, the calculated density is $1.896\ g/cm^3$. Sets of symmetry equivalent positions for Pnma are given in Table II.

TABLE II.

Symmetry Relations for Space Group

Pnma

(origin at $\bar{1}$)

Number of Positions	Wyckoff Notation	Point Symmetry	Coordinates of Equivalent Positions	Conditions Limiting Reflections
8	d	1	x,y,z; $\frac{1}{2}+x,\frac{1}{2}-y,\frac{1}{2}-z$; $\bar{x},\frac{1}{2}+y,\bar{z}$; $\frac{1}{2}-x,\bar{y},\frac{1}{2}+z$	0kl: k+l = 2n
			$\bar{x},\bar{y},\bar{z}$; $\frac{1}{2}-x,\frac{1}{2}+y,\frac{1}{2}+z$; $x,\frac{1}{2}-y,z$; $\frac{1}{2}+x,y,\frac{1}{2}-z$	hk0: h = 2n
4	c	m	$x,\frac{1}{4},z$; $\frac{1}{2}-x,\frac{3}{4},\frac{1}{2}+z$; $\frac{1}{2}+x,\frac{1}{4},\frac{1}{2}-z$	
4	b	$\bar{1}$	$0,0,\frac{1}{2}$; $0,\frac{1}{2},\frac{1}{2}$; $\frac{1}{2},0,0$; $\frac{1}{2},\frac{1}{2},0$	hkl: h+l = 2n k = 2n
4	a	$\bar{1}$	$0,0,0$; $0,\frac{1}{2},0$; $\frac{1}{2},0,\frac{1}{2}$; $\frac{1}{2},\frac{1}{2},\frac{1}{2}$	

C. Structure Determination

Diffraction data were collected on a Picker automatic diffractometer using Mo-Kα radiation, λ = 0.7107 Å. Six high angle reflections centered at a 3° take-off angle were used as the basis for a least squares refinement to give the final cell constants, which are tabulated in Section B.

Intensities of the form $hk\ell$, $\bar{h}k\ell$, and $h\bar{k}\ell$ were collected for $2\theta \leq 55°$ using a $\theta - 2\theta$ scan at a rate of 1° per minute. Intensities of three strong standard reflections were collected every 150 reflections and showed no sign of decomposition during data collection.

A total of 2948 intensities were recorded which were averaged to give a data set of 960 independent reflections. I_{ave} is simply an arithmetic average, $I_{ave} = \Sigma I/N$, where N is equal to the number of reflections. The standard deviation, $\sigma(I_{ave})$, is calculated from the formula $\sigma(I_{ave}) = [\Sigma(\sigma^2)]^{\frac{1}{2}}/N$. Also, $S = [\sigma(\Sigma\delta^2)]^{\frac{1}{2}}/N\text{-}1$, where $\delta = (I_{obs} - I_{ave})$. The standard deviation, $\sigma(I_{ave})$, is used in all cases except when $S > \sigma$; in which cases the value for S is used.

Anomolous dispersion, Lorentz and polarization corrections were applied, and net intensity was calculated from the relationship:

$$I = C - (B_1 + B_2)(T_c/2T_b) ,$$

where C represents the total recorded counts in scan time T_c and B_1 and B_2 are background counts for time T_b. The standard deviation of the measured intensities is formulated as:

$$\sigma(I) = [C + (T_c/2T_b)^2(B_1 + B_2) + (qI)^2]^{\frac{1}{2}}$$

where q is an arbitrary value of 0.05 to prevent very small relative errors in large counts.

Values of F^2 and $\sigma(F^2)$ were calculated from I and $\sigma(I)$. By the method of finite differences, the sigma of the structure factor is determined from:

$$\sigma(F) = F_o - [F_o^2 - S\sigma(I)/Lp]^{\frac{1}{2}} ,$$

where S is the scaling factor in $F_o = (SI/Lp)^{\frac{1}{2}}$. When $I \leq \sigma(I)$, $\sigma(F)$ becomes $[S\sigma(I)/Lp]^{\frac{1}{2}}$. Refinements were carried out using Zalkin s unpublished version of a full-matrix least squares program which minimizes the function

$$R^2 = \Sigma w(|F_o| - |F_c|)^2 / \Sigma w|F_o|^2 .$$

F_o and F_c are magnitudes of the observed and calculated structure factors, and the weighting factor $w = [\sigma(F)]^{-2}$. Anisotropic temperature factors of the form

$$\exp(-\beta_{11}h^2 - \beta_{22}k^2 - \beta_{33}l^2 - 2\beta_{12}hj - 2\beta_{13}hl - 2\beta_{23}kl)$$

were used. The β_{ij} values reported are related to the β's in the above expression by the relation

$$U_{ij} = 4\beta_{ij}/ai^*aj^*,$$

in which ai* is the i^{th} reciprocal cell length. All atoms were considered to be in their neutral valence state, and Cromer's

scattering factors were used for all atoms.[31] No absorption correction was applied.

All calculations were done on a CDC-6600 computer using unpublished versions of least squares, FORDAP and other programs written and revised by A. Zalkin. Molecular and Stereoscopic drawings were done using Johnson's ORTEP program.[32]

Since there was evidence to support that $F_{11}XeRu$ is isostructural with the platinum compound on the basis of x-ray powder patterns and infrared spectra, initial atomic parameters were taken from the platinum structure.[21] Positions of the heavy atoms were verified from a three-dimensional Patterson analysis. A difference Fourier verified positions of the fluorines, showing six to be in a closely octahedral arrangement around the ruthenium atom. Three cycles of a full-matrix least squares refinement on 737 reflections having $I \geq 1\sigma$ yielded a residual index of $R = 0.083$. Allowing anisotropic parameters for the heavy atoms reduced the residual to 0.074. Finally, a full-matrix refinement with all atoms anisotropic gave an R of 0.062. At this point, limiting the refinement to the 556 reflections where $I \geq 3\sigma$ reduced R to a value of 0.042.

The intensity of one fluorine peak was determined from a final Fourier electron density map. The highest peak on a final difference Fourier proved to be only 0.04 the intensity of one fluorine peak taken from the Fourier, thus accounting for all atoms. Final positional parameters and temperature factors are given in Tables III and IV, interatomic distances are tabulated in Table V, and structural angles listed in Table VI.

TABLE III.

Final Positional Parameters* (Å)
with Estimated Standard Deviations

Atom	x	y	z
Ru	.54318(7)	1/4	.22046(24)
Xe	.34978(6)	1/4	.70090(23)
F(3)	.54174(39)	.47539(78)	.22713(146)
F(4)	.48802(64)	1/4	.51096(183)
F(5)	.59210(61)	1/4	-.06886(22)
F(6)	.63925(56	1/4	.37393(218)
F(7)	.44428(52)	1/4	.06797(167)
F(8)	.34575(50	.09389(83)	.46413(149)
F(9)	.31279(50)	.09554(90)	.91147(157)
F(10)	.24562(56)	1/4	.62895(267)

*in fractional cell coordinates.

TABLE IV.

Anisotropic Thermal Parameters (multiplied by 10^3) in $Å^2$
and Estimated Standard Deviations

Atom	β_{11}	β_{22}	β_{33}	β_{12}	β_{13}	β_{23}
Ru	2288(53)	1832(46)	2116(58)	0	-1715(44)	0
Xe	2094(44)	3164(47)	2926(55)	0	-3717(37)	0
F(3)	5043(351)	2256(246)	4296(353)	-3118(227)	-7933(295)	5958(275)
F(4)	3568(492)	3753(424)	2575(465)	0	-97(347)	0
F(5)	3185(490)	5756(582)	4242(625)	0	1281(429)	0
F(6)	2122(415)	4252(467)	4673(615)	0	-6300(367)	0
F(7)	2946(435)	3206(389)	2121(395)	0	-3067(317)	0
F(8)	6074(480)	3449(326)	3614(379)	0	-1639(317)	0
F(9)	5795(437)	4323(382)	4800(438)	-8672(308)	925(329)	8310(319)
F(10)	1294(389)	7296(694)	8357(863)	0	-2292(465)	0

TABLE V.

Interatomic Distances (Å)
and Their Standard Deviations

Bond	Distance
Ru - F(3)	1.850(7)
Ru - F(4)	1.876(11)
Ru - F(5)	1.820(12)
Ru - F(6)	1.827(10)
Ru - F(7)	1.867(9)
Xe - F(3)	2.924(7)
Xe - F(4)	2.552(11)
Xe - F(7)	2.601(9)
Xe - F(8)	1.848(8)
Xe - F(9)	1.841(8)
Xe - F(10)	1.793(8)

TABLE VI.

Interatomic Bond Angles
and Their Standard Deviations

Angle	Degrees
F(3)-Xe-F(10)	129.59(.30)
F(8)-Xe-F(8')	87.78(.25)
F(8)-Xe-F(9)	88.44(.41)
F(8)-Xe-F(10)	78.59(.43)
F(7)-Xe-F(10)	140.57(.65)
F(4)-Xe-F(10)	142.26(.69)
Ru-F(7)-Xe	154.86(.29)
Ru-F(3)-Xe	139.91(.22)
Ru-F(4)-Xe	144.26(.34)
F(4)-Ru-F(7)	87.76(.53)
F(4)-Ru-F(6)	91.40(.61)
F(5)-Ru-F(6)	91.36(.56)
F(5)-Ru-F(7)	89.48(61)
F(6)-Ru-F(7)	179.16(.81)
F(4)-Ru-F(5)	177.24(.79)

IV. RESULTS AND DISCUSSION

A. Description of $F_{11}XeRu$ Structure

Final values of atomic positions and calculated bond angles are consistent with the cation and anion formulation $XeF_5^+RuF_6^-$ as shown in Figures 3 and 4. A stereoscopic drawing can be found in the Appendix, Figure 5.

Six fluorine atoms around ruthenium form a slightly distorted octahedron, the Ru-F bond lengths ranging from 1.83(6) to 1.88(5) Å, and the angles ranging from 88° to 91°. The two Ru-F short bonds are trans to the elongated bridges. Most probably the octahedral RuF_6^- anion exhibits this slight distortion because certain fluorine atoms of the RuF_6^- group are attracted more strongly than others to the xenon atoms.

The xenon is surrounded by five close fluorines in a square pyramidal arrangement. Xenon sits slightly below the planar base of this pyramid, making the cation umbrella shaped; the angle F_{axial}-Xe-F_{basal} is less than 90°. The four basal Xe-F bonds are approximately equal in length, but the apical Xe-F distance is significantly shorter, 1.79(8) Å.

The XeF_5^+ ion is coordinated to four RuF_6^- anions. One fluorine atom of each RuF_6^- is bridging to xenon. The four bridging fluorines are so arranged as to avoid the four-fold axis of the XeF_5^+, indicating that a sterically active lone pair lies along that axis. This is consistent with an isolated cation having a molecular geometry very similar to its isoelectronic relative, IF_5, as illustrated in Table I.

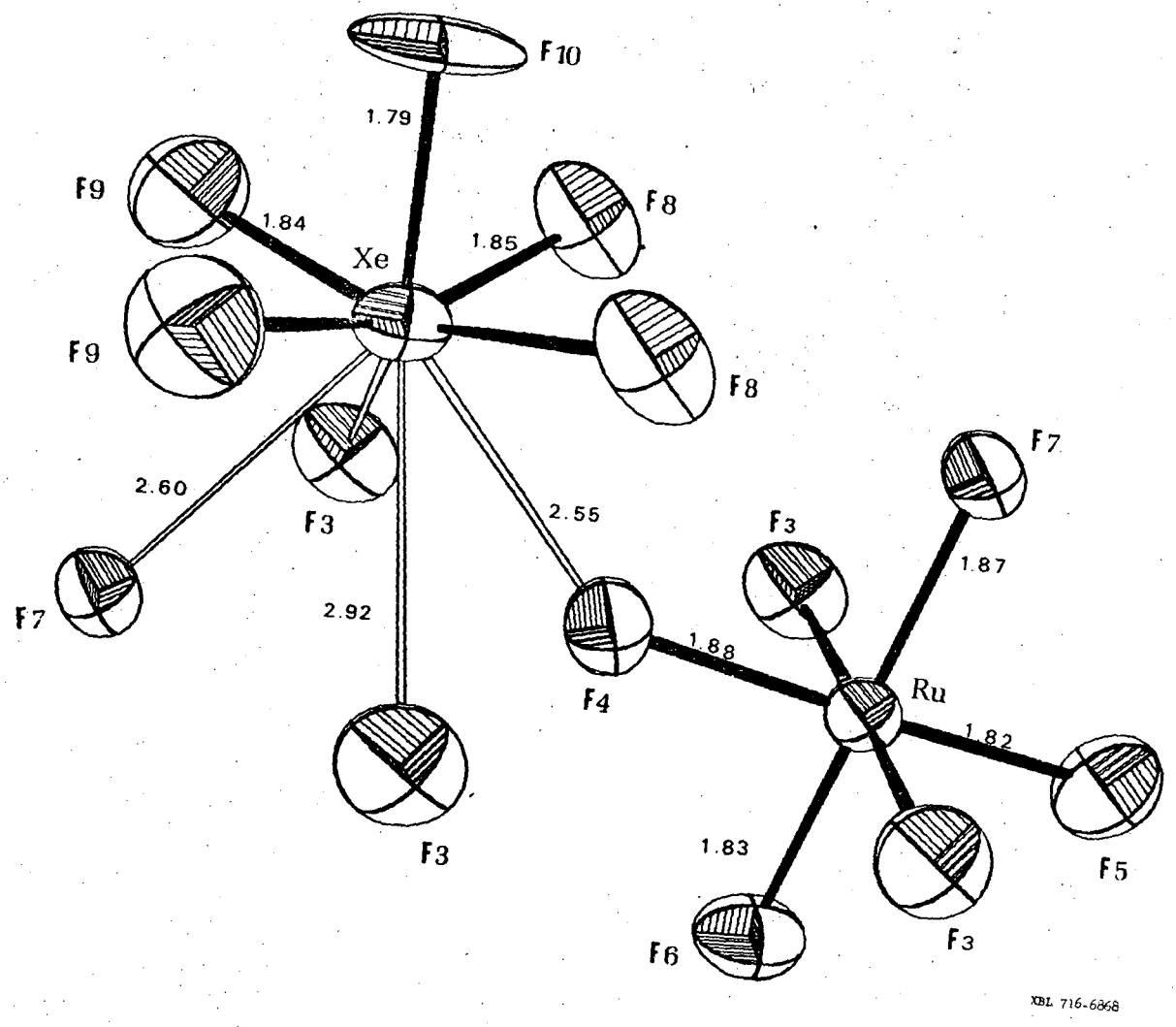
F10
1.79
F9
1.84
Xe
1.85
F8
F9
F8
2.60
F3
2.55
F7
F3
1.87
F7
2.92
1.88
F4
Ru
1.82
F5
1.83
F3
F6
F3
XBL 716-6868

Figure 3

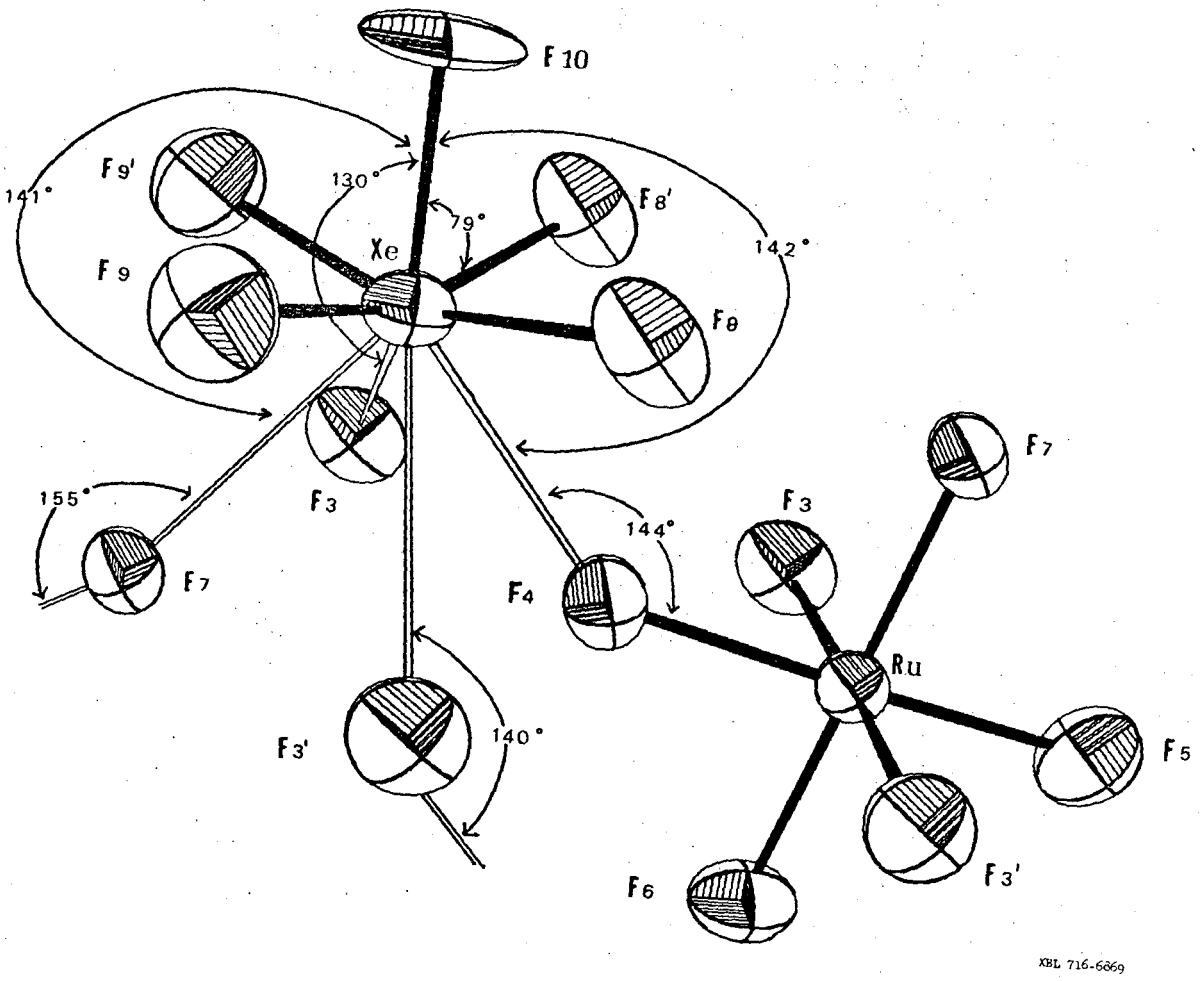
F 10
F 9'
141°
130°
79°
F 8'
Xe
F 9
142°
F 8
F 3
155°
F 7
144°
F 4
F 3
F 7
Ru
F 5
F 3'
140°
F 3'
F 6
XBL 716-6869

Figure 4

The fluorine bridge interactions are of interest. Two of these, F(3) and F(3'), are fluorine atoms which have like species in trans position in the RuF_6^- group. The other two bridging fluorine atoms, F(4) and F(7), are in cis relationship in the RuF_6^-. It is notable that the cis related bridging fluorine atoms make closer contacts with the xenon atom.

The xenon coordination includes, therefore, nine fluorine atoms, ten if the non-bonding electron pair is also included, as illustrated in the figure below.

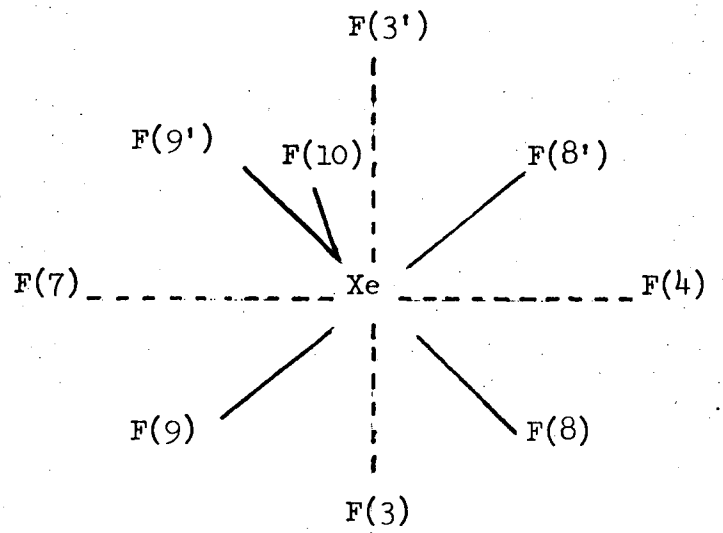

The geometry is essentially that of a capped Archimedian antiprism.

An interesting feature of the XeF_5^+ cation is the high thermal motion of the axial fluorine in the plane parallel to that of the basal fluorines. The anisotropic temperature factor in the β_{11} plane is 7.295 as compared to a value of 1.294 for thermal motion in the β_{22} plane. In other words, that axial fluorine is greatly constrained to vibrate only in one plane. Johnson's ORTEP[30] program represents this thermal motion by an ellipsoidal shape based on 50% probability. A more realistic picture of the shape of this high thermal motion was obtained from a crude hand plot of electron density taken from a Fourier analysis in the region of the axial fluorine. Looking down the F(10)-Xe bond, the thermal motion of F(10) avoids the area of the basal fluorines:

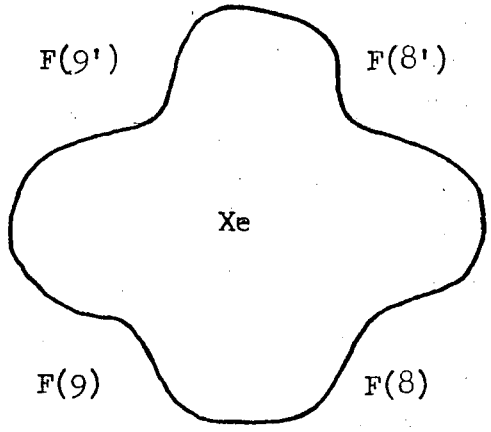

The packing diagrams shown in Figure 6 and in Figure 7 of the Appendix somewhat illustrate the constraining effects imposed on the axial fluorine by other surrounding atoms.

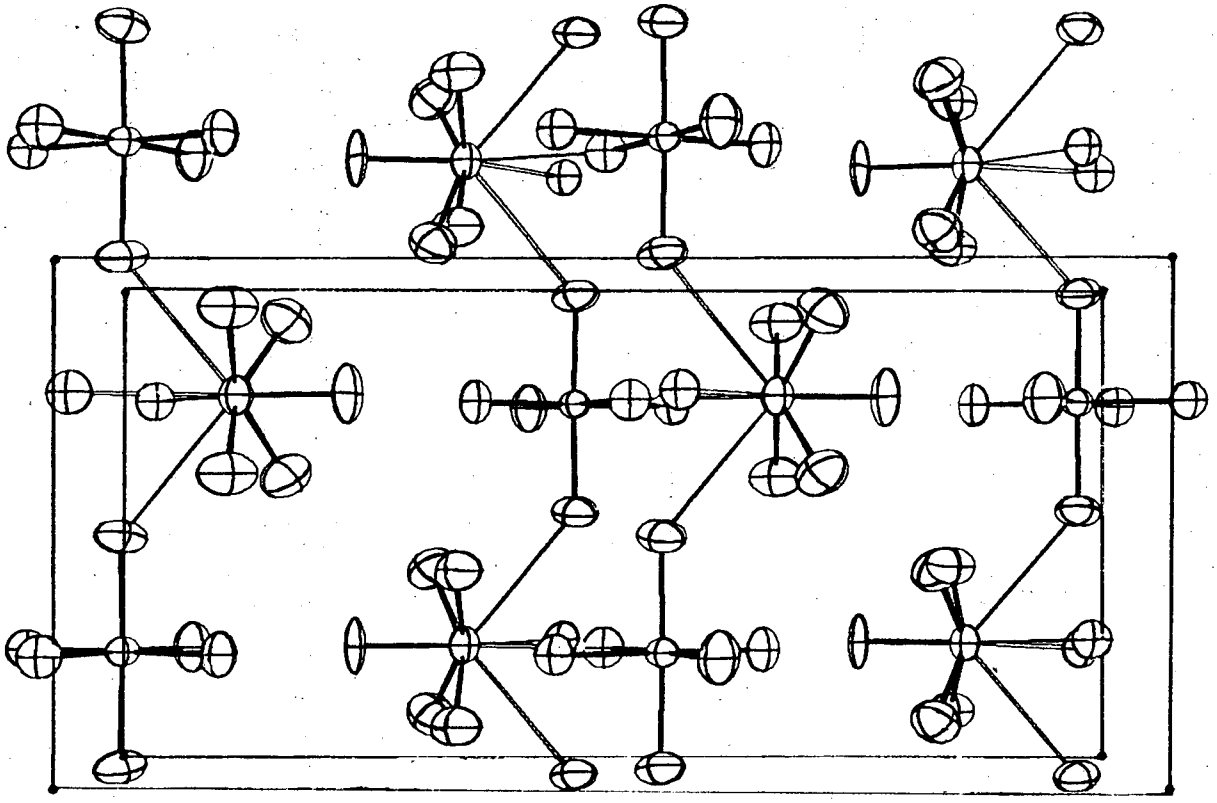

XBL 716-6871

Figure 6

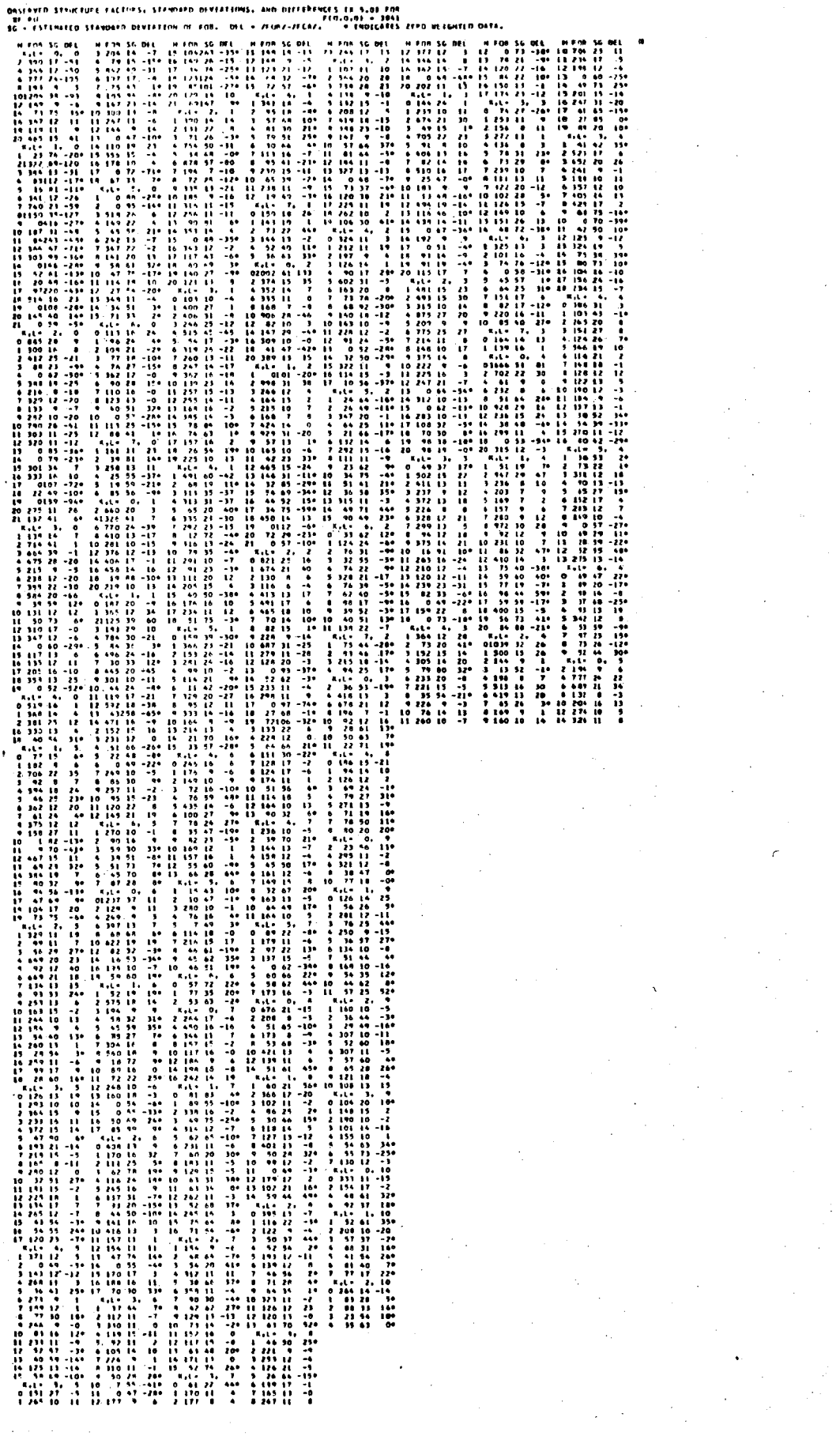

Figure 8. Comparison of calculated and observed structure factors.

B. Bonding Models Compatible with XeF_5^+ Geometry

1. Electron pair repulsion model. Gillespie's valence shell electron pair repulsion theory[33] assumes that each fluorine bond to the xenon involves an electron pair and that all non-bonding valence electron pairs have steric effect. Basic to the theory is the condition that the repulsion of non-bonding electron pairs is greater than repulsion of bonding electron pairs. Electron pair separation is thus maximized. XeF_5^+ has six electron pairs, five bonding and one non-bonding. Using this theoretical model, the XeF_5^+ cation is viewed as a pseudo octahedron, the non-bonding valence electron pair occupying one of the octahedral sites and each Xe-F bond involving a bonding electron pair. The repulsion of the one non-bonded electron pair tends to repel the four basal Xe-F bonding electron pairs by pushing them up and out. This accounts for the F_a-Xe-F_b angles of less than 90° and the F_b-Xe-F_b angles of less than 180°.

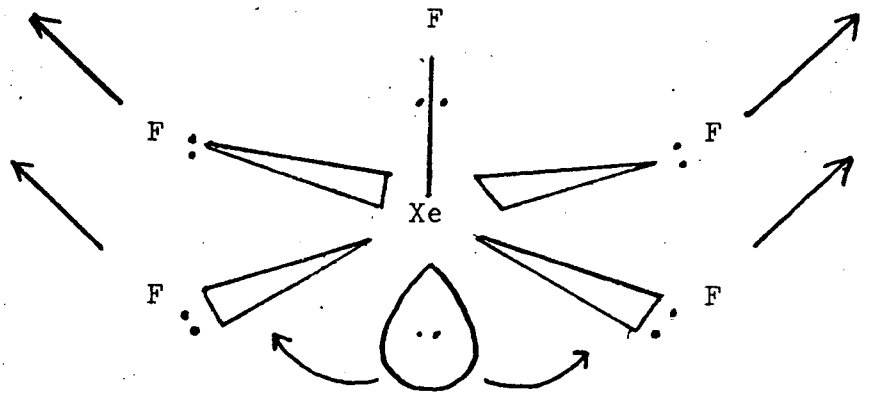

In addition, since the unique fluorine bonding electron pair interacts at about 90° with four bonding electron pairs, whereas each fluorine atom of the square planar arrangement interacts with one non-bonding pair plus three bonding pairs, the repulsion experienced by the latter basal fluorine bond pairs is greater than for the axial fluorine. Consequently, the valence electron pair repulsion theory also suggests a somewhat shorter axial bond and thus is compatible with the observed XeF_5^+ cation geometry.

2. Molecular orbital treatment. Simple molecular orbital treatments of the bonding in xenon fluorides as proposed by Pimentel[34] and Rundle[35,36] involve only 5s and 5p orbitals of the valence shell to form sigma-type bonds. These and other authors hold that the use of orbitals higher than valence shell is unlikely in view of very high promotional energy.[37,38,39]

In the case of XeF_5^+, three 3-center molecular orbitals are generated from the xenon $5p_x$ and a $2p_x$ orbital of each fluorine ligand in co-linear disposition. The xenon atom contributes two electrons and each fluorine contributes one electron to this p-sigma system, leaving the antibonding molecular orbital empty.

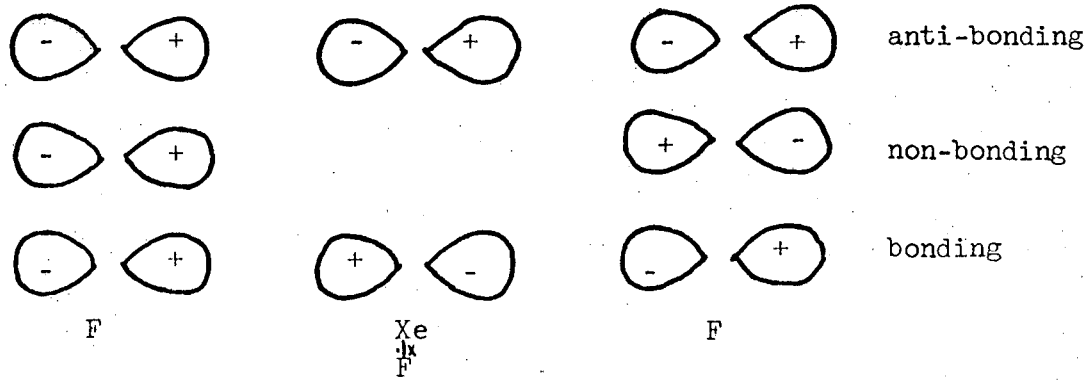

As shown in the diagram, two electrons occupy the bonding 3-center molecular orbital, and two occupy the nonbonding molecular orbital. The latter places electron density primarily on the fluorine atoms. This gives the Xe-F bond semi-ionic character,[40] the xenon atom being positively charged and the fluorine atom negatively charged.

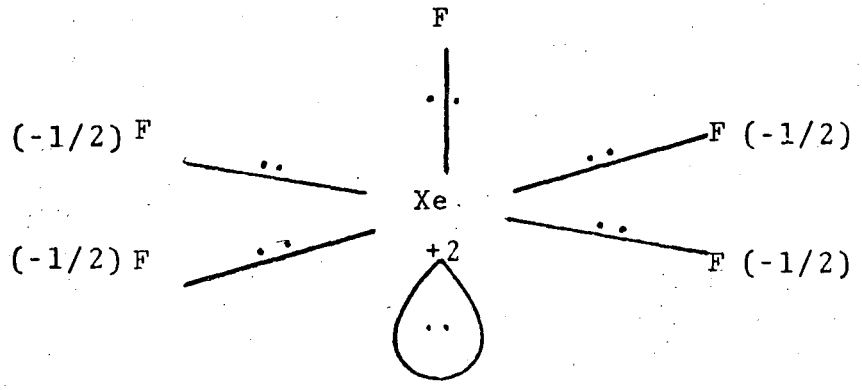

Thus, the unique fluorine atom is considered bound to the xenon atom by a conventional electron pair bond and pairs of opposite fluorine atoms in the square base are bound by weaker 3-center 4-electron bonds.

Although the polarity will enhance the bonding on the three-center bonds, there is, nevertheless, the expectation from this model that the F_{axial}-Xe electron pair bond will be stronger (hence shorter) than the F_{eq}-Xe bonds. This three-center bonding is ideally characterized with a linear F-Xe-F bond. In this structure, however, the angles of this bond are less than 180° as predicted by valence electron pair repulsion theory.

3. Bilham and Linnett Model. The bonding model proposed by Linnett and Bilham[41] is very similar to the electron-pair repulsion model described earlier. Instead of describing Xe-F bonds as electron pairs, however, Linnett's description of the XeF_5^+ species includes two electron pairs, the axial Xe-F bond and the non-bonding electron pair, and four one-electron Xe-F equatorial bonds.

Such a picture of electronic structure is developed on the basis that each atom will have an octet of electrons composed of two spin sets of four. Normally, to minimize electron repulsion, each spin set of four is tetrahedral, but Linnett relaxes this condition somewhat for heavier atoms.

In the case of the XeF_5^+ cation, we can formulate a Linnett representation by beginning with the $\cdot\times\underset{\times\cdot}{\overset{\cdot\times}{\times\cdot Xe\cdot\times}}\ F^+$ electron-pair bound species. To this add four fluorine atoms, each atom acquiring a share in a xenon electron: $Xe\bullet \rightarrow F$. Thus, of the eight xenon electrons we can visualize two (a spin pair) donated to F^+ and four (singly) donated to four fluorine atoms and a non-bonding spin pair remains. The geometry anticipated for the group XeF_5^+ is then one derived from the six electron-group array: one non-bonding electron pair, one bonding pair, four single electron species.

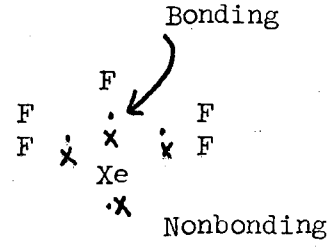

The geometry which places the electron pairs trans in an octahedron appears to be the most favorable. Thus, a square-based pyramid geometry is again suggested. As in the electron-pair repulsion picture, the equatorial fluorine ligands will be pushed upwards by the non-bonding electron pair. Furthermore, the F_{eq}-Xe bonds should be more polar; and also, since they are single electron bonds, should be weaker than the F_{axial}-Xe bond. The Bilham and Linnett model, therefore, has in it elements of both other models.

4. Valence bond model. In constructing a valence bond model[42] for the bonding in XeF_5^+, we begin by determining the ionic formulation that will give the maximum number of possible valence bonds, namely, three. This ionic formulation is $[XeF_3]^{3+}[2F]^-$. $[XeF_3]^{3+}$, like SbF_3, has a pyramidal structure and preserves the octet around xenon. This ionic description provides the maximum number of possible resonance forms with the observed geometry if the two fluoride ions are attached symmetrically:

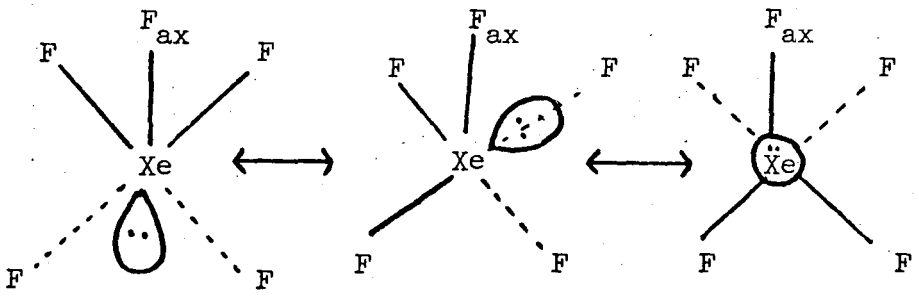

Here the axial Xe-F bond is an electron-pair bond, and the two fluoride ions make their approach along an axis co-linear to the Xe-F bond in the pyramidal XeF_3^{3+} ion in order to generate maximum

resonance energy. The equatorial Xe-F bonds are the resonance hybrids of $(F\text{-}Xe)^{+}\cdots\cdot F^{-}$, and $F^{-}\cdots\cdot(Xe\text{-}F)^{+}$ pairs.

Thus, as in the Pimentel-Rundle and Linnett models, the F_{eq}-Xe will be a semi-ionic, single electron bond, and similar expectations apply to the XeF_5^{+} geometry. Interestingly, all models, including the valence electron pair repulsion model, are consistent with the observed cation geometry. Since the F_{ax}-Xe bond length is not markedly shorter than the F_{eq}-Xe length, the theories must be made much more quantitative for a good choice to be made.

C. Fluoride Ion Donor Properties of XeF_6 with RuF_5

Earlier work has shown that XeF_6 is superior to XeF_2 as a fluoride ion donor.[15] The previously described work helps to support the view that the XeF_6 adducts with fluoride ion acceptors are XeF_5^+ salts. XeF_4 does form compounds with the best fluoride ion acceptor, SbF_5[43] but no evidence for the XeF_3^+ ion presently exists.

The extremely good donor properties of XeF_6 and the peculiar stability of the pseudo-octahedral geometry of the XeF_5^+ cation are compatible with the enthalpies of ionization associated with these reactions.[44]

Our experiments in the $XeF_5^+RuF_6^-/XeF_2$ system support the earlier contention that XeF_2 is not capable of displacing XeF_6 from its salts. Furthermore, xenon difluoride does not form an adduct with XeF_5^+ in the RuF_6^- case. Although there is no satisfactory explanation to account for the absence of an adduct here, in contrast to the $XeF_5^+AsF_6^-$ behavior, it may be correlated with the fact that the anion in one case is a transition metal MF_6^- and in the other case not. d-Orbitals on the ruthenium can provide for pi-bonding of the fluorine ligands of RuF_6^-, whereas in AsF_6^- adducts this is less likely to be so. This may be the reason why the XeF_5^+ cation in $XeF_5^+RuF_6^-$ is coordinated to four RuF_6^- ions, whereas in $XeF_5^+AsF_6^-$ there are three bridging fluorine atoms (of the anion). Of course, the difference in coordination of the XeF_5^+ in the two cases may also be responsible for the difference in XeF_2 adduct formation.

ACKNOWLEDGEMENTS

I express sincere appreciation to my research director, Professor Neil Bartlett, for his continued interest and encouragement throughout the course of this work. I am especially indebted to him for opening my eyes to the many facets of science.

For his expert guidance and lucid explanations, I thank Dr. Allan Zalkin for what proved to be a most rewarding introduction to crystallography. Along with many helpful suggestions, discussions with D. D. Gibler and other members of the Bartlett research group were greatly enlightening to this project and to my graduate education at Berkeley.

Finally, I am grateful to my husband Dennis for providing a constant source of moral support and encouragement.

This work was supported by the Atomic Energy Commission.

APPENDICES

Figure 5. Stereoscopic drawing of the $XeF_5^+RuF_6^-$ unit.

Figure 7. Stereoscopic packing diagram of 1.5 unit cells of $XeF_5^+RuF_6^-$.

These stereoscopic drawings were done using Johnson's ORTEP program.

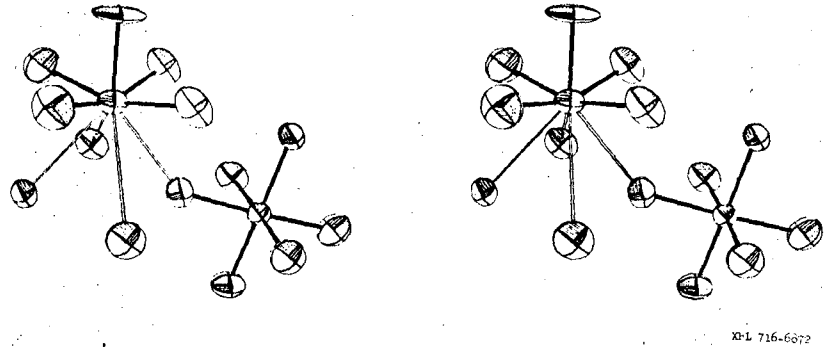

XBL 716-6872

Figure 5

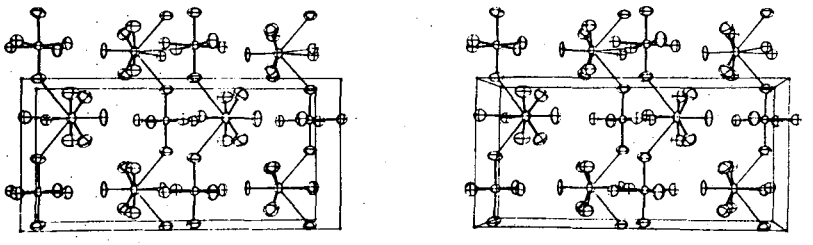

Figure 7

REFERENCES

1. N. Bartlett, Proc. Chem. Soc. 1962, 218.

2. N. Bartlett and F. O. Sladky, "The Chemistry of Krypton, Xenon, and Radon, UCRL-19658, June, 1970.

3. JANAF Thermochemical Tables, Dow Chemical Company, Midland, Michigan, (Dec., 1960, to Dec., 1969).

4. See reference 2.

5. C. L. Chernick, H. H. Claassen, P. R. Fields, H. H. Hyman, J. G. Malm, M. W. Manning, M. S. Matheson, L. A. Quarterman, F. Schreiner, H. H. Selig, I. Sheft, S. Siegel, E. N. Sloth, L. Stein, M. H. Studier, J. L. Weeks, and M. H. Zurin, Science 138, 162 (1962).

6. R. Hoppe, W. Dahne, H. Mattauch, and K. M. Rodder, Angew. Chem. 74, 903 (1962).

7. J. L. Weeks, C. L. Chernick, and M. S. Matheson, J. Amer. Chem. Soc. 84, 4612 (1962).

8. R. Hoppe, H. Mattauch, K. M. Rodder, W. Dahne, Z. Anorg. Chem. 324, 214 (1963).

9. D. F. Smith, J. Chem. Phys. 38, 270 (1963).

10. H. H. Claassen, H. Selig, and J. G. Malm, J. Amer. Chem. Soc. 84, 3593 (1962).

11. E. E. Weaver, B. Weinstock, C. P. Knop, J. Amer. Chem. Soc. 85, 111 (1963).

12. J. Slivnik, Croat. Chem. Acta. 34, 253 (1962).

13. J. G. Malm, I. Sheft, and C. L. Chernick, J. Amer. Chem. Soc. 85, 110 (1963).

14. F. B. Dudley, G. Gard, and H. Cady, Inorg. Chem. 2, 228 (1963).

15. N. Bartlett and F. O. Sladky, J. Amer. Chem. Soc. 90, 5316 (1968).

16. H. Selig, Science 144, 537 (1964).

17. N. Bartlett, S. P. Beaton, and N. J. Kha, Abstracts, 148th National Meeting of the ACS, Chicago, Illinois; August-September, 1964, No. K3.

18. K. E. Pullen and G. H. Cady, Inorg. Chem. 6 , 2267 (1967).

19. G. L. Gard and G. H. Cady, Inorg. Chem. 3, 1745 (1964).

20. N. Bartlett, F. Einstein, D. F. Stewart, and J. Trotter, Chem. Communs. 1966, 550.

21. N. Bartlett, F. Einstein, D. F. Stewart, and J. Trotter, J. Chem. Soc. A, 1190 (1967).

22. K. E. Pullen and G. H. Cady, Inorg. Chem. 6, 1300 (1967).

23. N. Bartlett and D. Gibler, unpublished observation.

24. A. J. Edwards and M. A. Mouty, J. Chem. Soc. A, 703 (1969).

25. G. R. Jones, R. D. Burbank, and N. Bartlett, Inorg. Chem. 9, 2264 (1970).

26. D. H. Templeton, F. J. Hollender, N. Bartlett, and M. Wechsberg, unpublished observation.

27. N. Bartlett and M. Wechsberg, "The Xenon Difluoride Complexes $XeF_2 \cdot XeOF_4$; $XeF_2 \cdot XeF_6 \cdot AsF_5$ and $XeF_2 \cdot 2XeF_6 \cdot 2AsF_5$ and Their Relevance to Bond Polarity and Fluoride Ion Donor Ability of XeF_2 and XeF_6," UCRL-20572, April, 1971.

28. N. Bartlett and N. K. Jha, "The Xenon-Platinum Hexafluoride Reaction and Related Reactions," in Noble Gas Compounds, Herbert H. Hyman, ed., (University of Chicago Press, 1963), p. 23.

29. F. O. Sladky, unpublished observation.

30. W. Garrison, unpublished observation.

31. D. T. Cromer and B. Mann, Acta. Cryst. A24, 321 (1968).

32. C. K. Johnson, ORTEP, Oak Ridge National Laboratory, June, 1965.

33. R. J. Gillespie, R. S. Nyholm, Quart. Rev. XI, 339 (1957).

34. G. C. Pimentel, J. Chem. Phys. 19, 446 (1951).

35. R. E. Rundle, J. Amer. Chem. Soc. 85, 112 (1963).

36. R. E. Rundle, Rec. Chem. Prog. 23, 195 (1962).

37. J. G. Malm, H. Selig, J. Jortner, and S. A. Rice, Chem. Revs. 65, 199 (1965).

38. C. A. Coulson, J. Chem. Soc. 1964, 1442.

39. See reference 28.

40. See reference 2.

41. J. Bilham and J. W. Linnett, Nature 201, 1323 (1964).

42. C. A. Coulson, Valence (Oxford University Press, New York) 2nd edition, (1961).

43. D. Martin, C. R. Acad. Sci. Paris C, 1145 (1969).

44. See reference 2.

TECHNICAL INFORMATION DIVISION
LAWRENCE BERKELEY LABORATORY
UNIVERSITY OF CALIFORNIA
BERKELEY, CALIFORNIA 94720